

Research Article

Experimental Research on Heating Transfer Improvement of Materials that Change Phase in Tunnels in Cold Regions

Xu Zhang ¹, Dianwei Qi ¹, Wanjiang Wang,¹ Jiaqi Zhang,¹ Hongchao Yan,² and Xiancheng Li ²

¹Institute of Building Engineering, Xinjiang University, Urumqi 830017, China

²Business school, Xinjiang University, Urumqi 830091, China

Correspondence should be addressed to Dianwei Qi; qidianwei@xju.edu.cn

Received 5 August 2022; Revised 14 September 2022; Accepted 7 October 2022; Published 24 March 2023

Academic Editor: Dongjiang Pan

Copyright © 2023 Xu Zhang et al. This is an open access article distributed under the Creative Commons Attribution License, which permits unrestricted use, distribution, and reproduction in any medium, provided the original work is properly cited.

In tunnel heating systems, phase change materials may minimize the consumption of conventional electric energy, which is very considerate in the field of tunnel heating in cold regions. Because of the phase change material's poor heat conductivity, its annual growth rate heat absorption and release is slower; thus, the majority of phase change heat storage systems must improve heat transmission. In this study, a spiral metal ring is implanted in the paraffin to improve heat transmission to achieve this objective using a concentric sleeve-type paraffin heat storage device as a medium. Experiments were performed out in order to determine the effects of heating rate, hot fluid flow rate, and the use of a spiral metal ring on the heat storage and release process of a thermal storage device. In comparison to the paraffin thermal storage device, the embedding of the spiral metal ring accelerates the internal thermal performance of the composite heat storage device, resulting in a more uniform temperature distribution. When the thermal radiation heating rate is 60°C, 65°C, or 70°C during the heat storage process, the heat storage time of the composite heating storage device is reduced by 59.2 percent, 44.4 percent, and 40.7 percent, respectively. When the ambient temperature is 26°C and the heat storage device's starting temperature is 65°C, the exothermic time is reduced by 22.6 percent.

1. Introduction

In China, 84% of the tunnels in cold regions suffer from the problem of freezing damage, but most of taken antifreezing measures are passive measures, and they have problems of poor operation effect and high energy consumption. With phase shift heat storage technology, solar energy can be used for tunnel heating systems, which can effectively reduce heating energy consumption [1]. owing to the benefits of an excessive heating storage concentration and a temperature that remains constant [2–5], phase change materials have become a research hotspot, making it have broad application prospects [6–10] in the fields of “peak shifting and valley filling” [11–13], waste heat recovery [14–16], industrial and civil building heating [17–20], and solar heating system [21–25]. Besides, the main disadvantage the poor

heat capacity of the phase change heating storage system conductivity leads to a low rate of heat absorption and release, so it is essential to strengthening heat transfer in most heat storage systems. The current research about the primary goal of phase change heating storage systems would be accelerate the phase change heat transfer process.

Many scholars add fins [26–30] on the surface of the heat exchange tube to expand the trading space, and its impact of strengthening heat transfer is obvious. Ma [31] studied the impact of the number of fins on the phase change device's heat transfer performance using numerical simulation. It was discovered that when natural convection is disregarded, expanding the amount of fins on a phase change energy storage device will enhance its heat storage efficiency, but after a certain point, the rise in heating storage efficiency will cease and gradually decreases, indicating that

there is a limit to the amount of improvement that can be made.

Yuichi et al. [32], Zhu et al. [33], and Lei et al. [34] embedded nonmetallic materials with a high heat conductivity as the enhanced heat transfer medium, such as carbon fibers, silicon powder, and expanded graphite, in phase change materials by use of tests. The findings demonstrate that after embedding with the reinforcing medium, the composite phase change material's overall heat conductivity was significantly increased, the internal temperature distribution of the heat storage device became more uniform, and the time between heat storage and release was significantly decreased.

Compared with the powder nonmetallic material, more researchers choose to embed metal materials using phase change materials. In metal foam integrated by Siahpush et al. [35–38], the phase-changing materials effectively increases the heat conduction of the composite stage change materials to reduce the time needed for thermal storage and release. Among them, in the experiment by Liu et al. [38], adding copper foam reduced the heat storage time by 47.5%, which is due to the fact that, in addition to having a high heat transfer performance, metal foam also has a very large surface area per unit volume. The voids can also absorb more phase change materials. It increases the thermal area between the metal foam and the phase change substance and helps to boost heat transfer.

The ideal metal-enhanced heat transfer medium should have the advantages of being relatively cheap, small in size, easy to operate, and better in enhancing the heat transfer effect [39–42]. In this paper, a concentric casing type paraffin phase change heat storage test bench is designed, and a spiral metal ring is made of ordinary thin iron wire and embedded in the paraffin. In order to verify that the flow rate of the heat transfer fluid has little effect on the heat storage process to a certain extent, the low thermal conductivity of the phase change material is the key to limiting the heat storage rate. Considering that the heat source temperature has a great influence on the heat storage process, the experiment will also analyze the heat storage process under different heat source temperatures. The internal temperature rises features of the heat conduction and memory stick enhancement; the spiral metal ring's influence on the paraffin phase transition was mainly analyzed experimentally [43–46].

2. Materials

2.1. Paraffin. The heat storage material in this experiment is paraffin; before the experiment, the paraffin was analyzed by DSC 214 Polyma differential scanning calorimetry. Figure 1 shows the DSC a paraffin wax curves, it is clear that paraffin wax melting is a continuous heating process, and a phase transition endothermic peak appears when the temperature is 59.6°C. The intersection between the tangent line of the curve from stationary to the beginning of decreasing and the tangent line of the curve with the highest slope was taken as the initial temperature of paraffin transformation 53.6°C, and the temperature at the point where the curve became stationary again was the end temperature of phase transformation 62.6°C. The ratio of the area enclosed between the

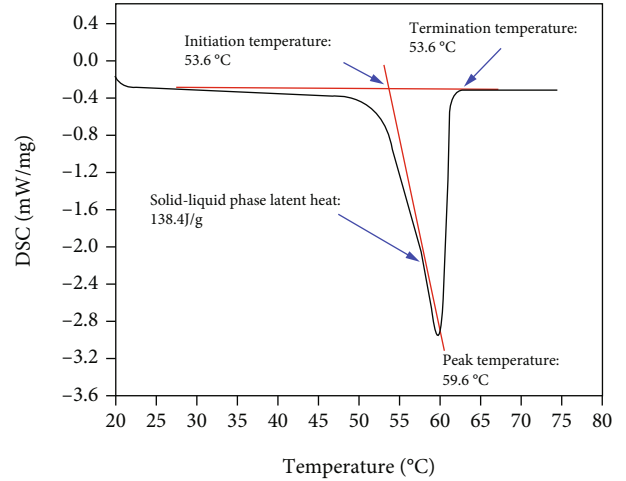


FIGURE 1: Paraffin DSC curve.

TABLE 1: The thermophysical properties of paraffin wax.

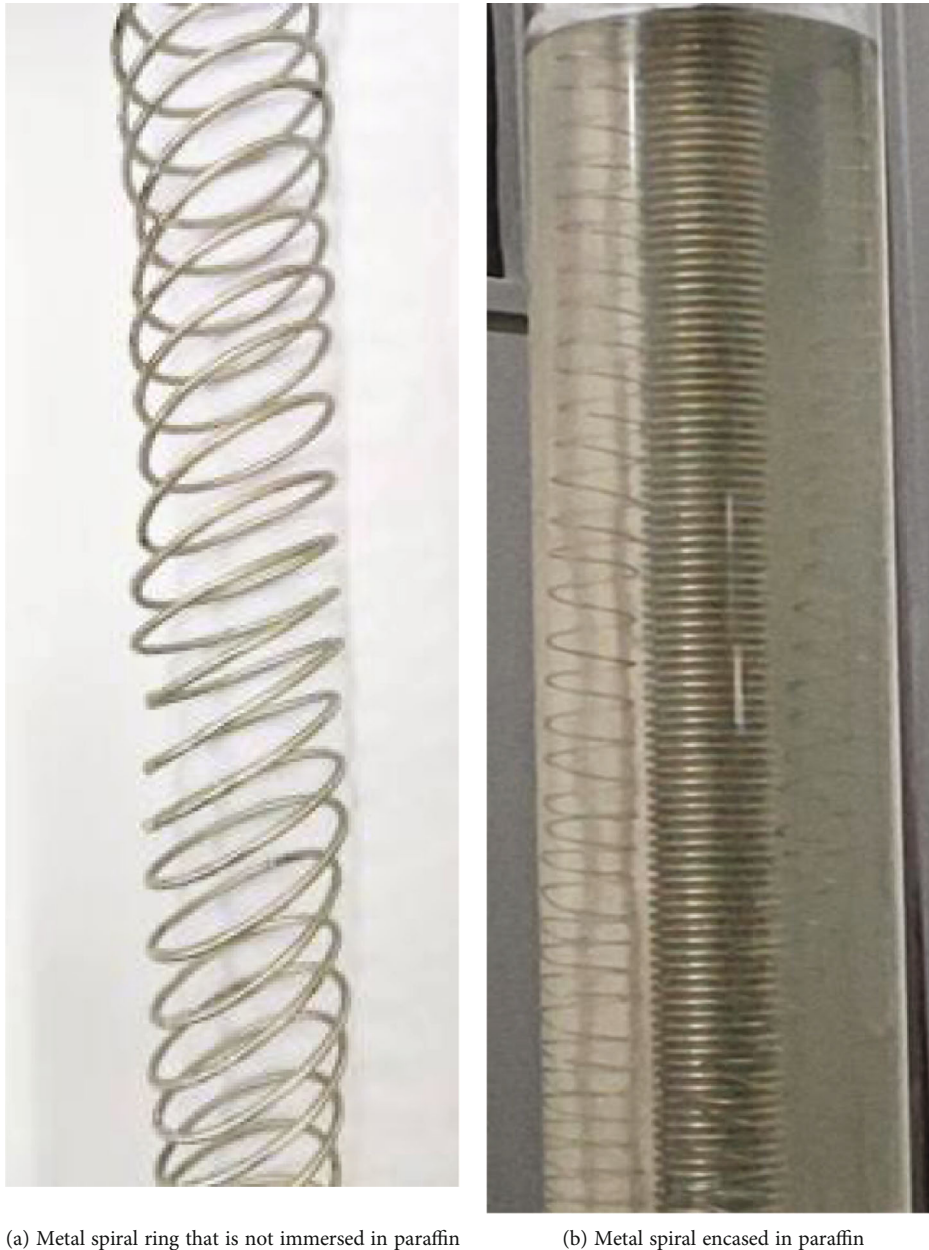
Span	Melting level (°C)	Density quantiles (m ³)	Heat conductivity (W/(m·K))	Concealed heating of phase transition (J/g)
Solid phase	53.6-	940	0.4	138.4
Liquid phase	62.6	760	0.15	

curve and the two tangent lines to the rate of temperature change is defined as the latent heat of the paraffin phase transition of 138.4 J/g. Thermodynamic characteristics of paraffin are indicated in Table 1.

2.2. Spiral Metal Ring. Making the paraffin-embedded improved heat transfer medium have the advantages of simple operation, low cost, small volume, and high heat conductivity, ordinary metal iron wire with a diameter of 1 mm is selected as the raw material and wrapped on the outside of a circular tube with a diameter of 20 mm, making it into a spiral metal ring; the length of a single spiral metal ring is 900 mm, and the weight is 0.14 kg. Three spiral metal rings are arranged in the heat storage device at equal intervals and similar to the heat exchange tube's axial direction, followed by the paraffin being melted and poured into the heat storage device to immerse the spiral metal rings; after solidification, the metal ring-paraffin composite, a device for storing heat, is made. Within the composite heat storage system, the filling amount of paraffin is 5 kg, and the spiral metal ring is 0.42 kg. The helical metal ring embedded in paraffin is shown in Figure 2.

3. Methodology

3.1. Test Devices. Figure 3 depicts the experimental apparatus for storing heat from paraffin phase change. The three components of this system are a phase change heat storage



(a) Metal spiral ring that is not immersed in paraffin

(b) Metal spiral encased in paraffin

FIGURE 2: Spiral metal ring.

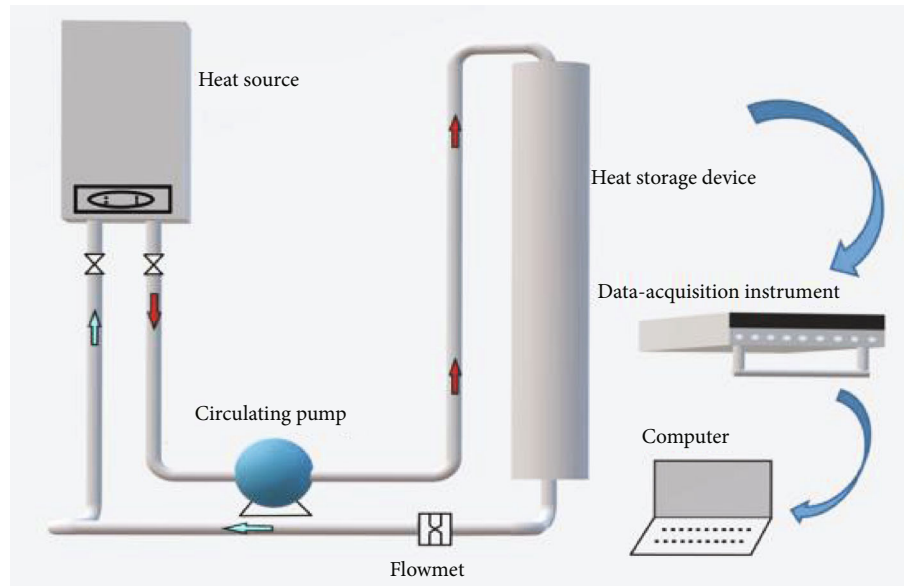
device, a water heating circulation system, and a temperature acquisition system.

The phase-transition thermal reservoir's outside casing is made of a cylindrical piece of Plexiglas with a height of 900 mm and an inner diameter of 90 mm. Its outer side is covered with a heat insulation material. The heat exchange tube is a spherical, and the stainless steel tube that is 900 mm long, 22 mm inside diameter, and 26 mm outside diameter. It runs top to bottom via the center of the heat storing device. Paraffin is put in the area between the inner wall of the heat storage device and the outer wall of the heat exchanger. A schematic of the phase change heat storage device is shown in Figure 4.

The water heating circulation system consists of an electric wall-hung boiler, circulating pump, and water flow

pipes. The electric wall-hung boiler is used to provide the heat source for the experimental system, and the circulating pump is used to provide power for the fluid circulation.

The temperature acquisition system consists of miniature high-precision thermocouples and an Agilent data acquisition instrument. As shown in Figure 5, three columns of temperature measuring points $L1$, $L2$, and $L3$ are positioned in the heat storage apparatus, and their distances from the inner wall of the heat storage device are 28 mm, 14 mm, and 0 mm, respectively; moreover, each column of temperature measuring points is equipped with 10 thermocouples at an equal distance of 100 mm to dynamically analyze the variation of temperature in paraffin phase transition process. After the thermocouple is calibrated, the measurement accuracy can reach 0.1°C , and the temperature data is automatically recorded every 5



(a) Schematic diagram of test system



(b) Schematic of the test system

FIGURE 3: Test system layout.

minutes by the Agilent data acquisition instrument and stored on the computer.

3.2. Research Content. In the process of heat storage, the electric wall-hung boiler is firstly turned on to make the heat fluid be heated to the set temperature. The hot fluid with a higher temperature passes through the heat storage device's heat exchange tube to warm the phase change substance paraffin. When almost no temperature difference exists between

the heat exchanger's input and exit, the heat source is shut off since it is believed to be the culmination of the heat storage. Once the heat storage process is over, the heat release process begins, during which the valve is switched to connect the circulating water to the end of the capillary tube, and the heat from the thermal storage device is released into the air via the capillary tube's end. When the temperature inside the heat storage device equals the temperature of the flowing water, the heat release ceases and the water circulation pump is switched

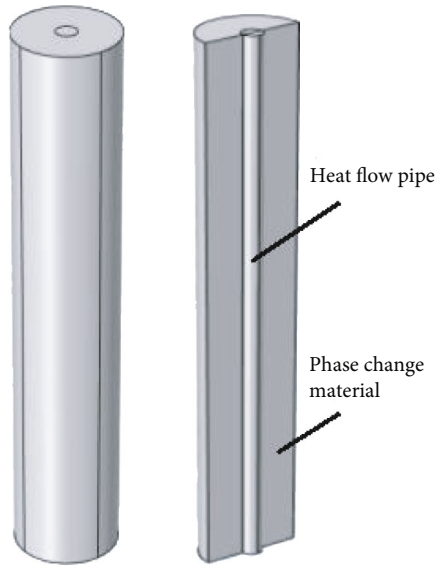


FIGURE 4: A phase change heat storage device shown schematically.

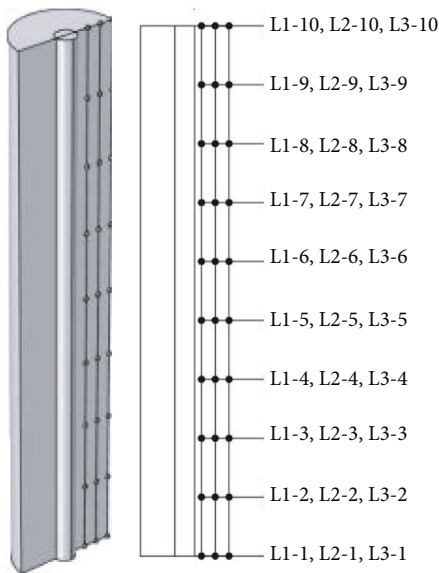


FIGURE 5: Schematic diagram of thermocouple arrangement.

off. To avoid errors, one group of the heat storage process carried out two times of experiments, as shown in Figure 6; in two experiments, the rising curves and trends of the temperature of almost overlap, which proves that the experiment is reliable and repeatable. (L1 is the average temperature of the ten measuring points in the first column, and L1 – 1 is the temperature of the first measuring point in the first column, the same meaning for L2 and L3.)

The following contents are studied in this paper: (1) the temperature change characteristics of the paraffin wax during its phase change; (2) the influence of different heat exchange fluid flow amount, different heat source temperatures, and different filling materials on how the heat storage gadget stores heat; and (3) the impact of various filler materials on the heat storage device’s ability to release heat.

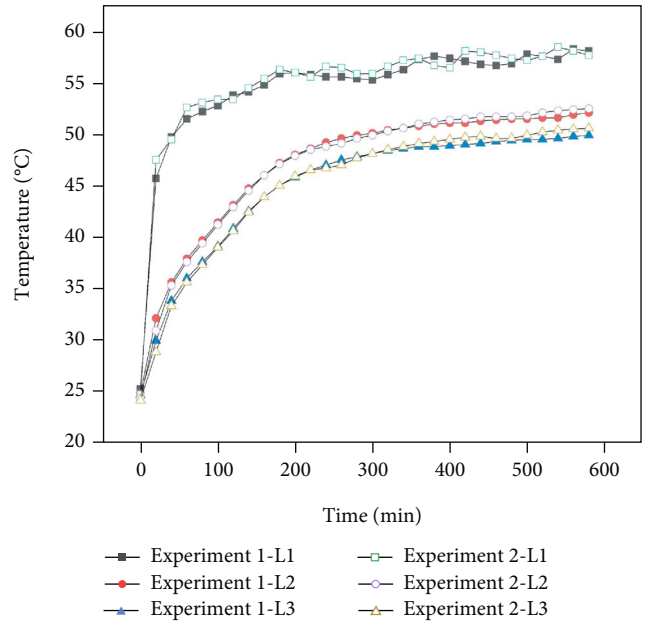


FIGURE 6: Repeated experiment.

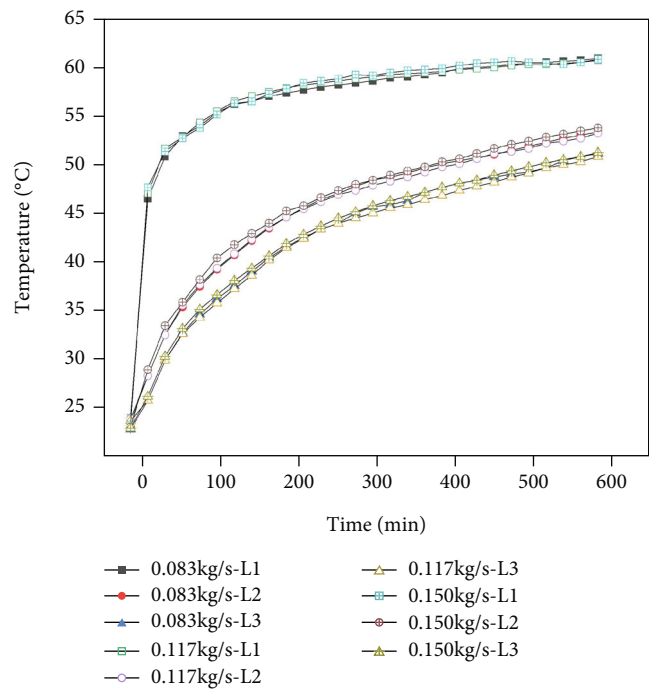


FIGURE 7: Temperature change of heat storage device under different heat flows and fluid flows.

4. Findings and Evaluation

4.1. Process for Storing Heat

4.1.1. Influence of Flow Amount of Heat Fluid on Paraffin Heat Storage Process. Figure 7 depicts the change in temperature inside the paraffin heat storing device the heat storage process with the heat source temperature set at 65°C and the

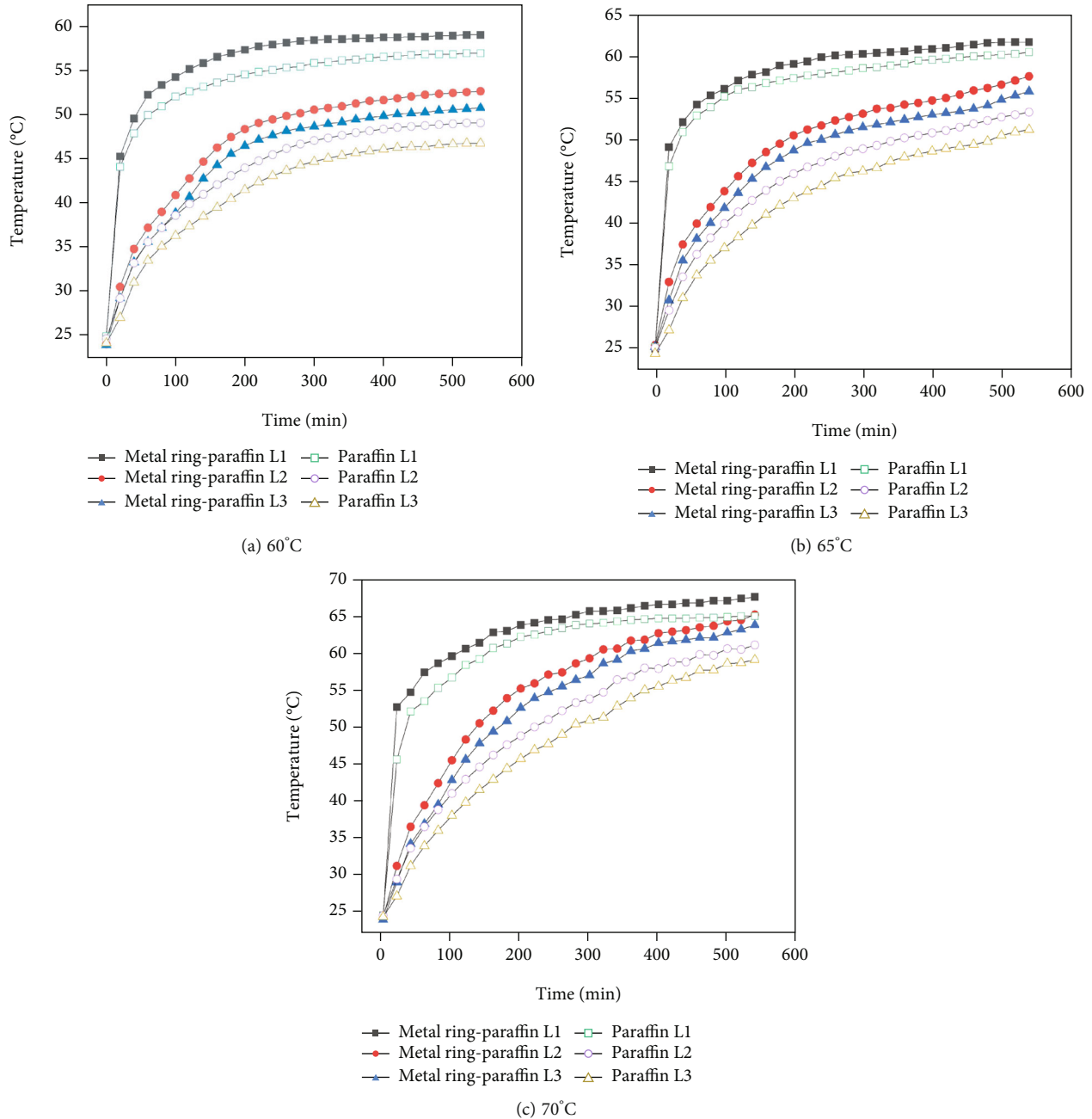


FIGURE 8: Temperature modifying the heat storage device dependent on the temperature of the heat source as well as filling material.

heat fluid flow rates of 0.083 kg/s, 0.117 kg/s, and 0.150 kg/s, respectively. Convective heat transfer works by forcing fluid to flow convectively within a tube, and while other variables are the same, this causes the flow rate (quantity) to rise in addition to the convective heat transfer coefficient of the inner wall of the tube, which strengthens convective heat transmission. Additionally, it is observed that when the flow rate of heat fluid in the paraffin heat storage device is 0.083 kg/s, 0.117 kg/s, and 0.150 kg/s, the change curves of paraffin temperature almost overlap during the heat storage process while the rate of heat storage does not increase as the flow amount increases. This is because the heat conductivity of the heat exchange tube in the test is 17 W/

(mK), but the heat conductivity of liquid paraffin is only 0.15 W/(mK). (The temperatures in the 1st, 2nd, and 3rd columns, respectively, are the average temperatures 10 measurement sites.)

4.1.2. Influence of Spiral Metal Ring on Paraffin Heat Storage Process. Figure 8 demonstrates the fluctuation in internal temperature embedded in the paraffin thermal storage device and the composite thermal storage device spiral metal ring at flow rates of 0.117 kg/s and heat source temperatures of 60°C, 65°C, and 70°C, respectively. Both paraffin heat storage devices and composite heat storage devices go through two phases in the process of storing heat: the sensible heat

absorption stage of the phase change substance and the latent heat absorption stage. Figure 8(c) demonstrates that, after the commencement of heat storage, paraffin wax temperature rapidly rises to its melting temperature, which is the stage of absorbing sensible heat; in the range of about 53°C–63°C, the paraffin absorbs the latent heat of phase transition, and the temperature rises slowly, which is consistent with the DSC curve. It is evident from Figure 8(a) that for both a paraffin heat storage device and a composite heat storage device embedded with a spiral metal ring, the temperature of L1 is always greater than that of L3, and the large temperature difference between L1 and L3 indicates that the internal temperature of the heat storage device exists a large inhomogeneity in the horizontal direction. It is also obvious from Figures 8(b) and 8(c) that this inhomogeneity is lessening as the heat source's temperature rises.

Figure 9 indicates that when L1 and L3 temperatures inside various heat storage devices are compared at various heat source temperatures. At the same thermal source temperature, the temperature differential in the horizontal direction of the composite thermal storage device is less than that of the paraffin heat storage device. When the heat source is 60, 65, or 70 degrees Celsius, the temperature difference between L1 and L3 is utilized to measure the temperature inhomogeneity in the horizontal direction of the heat storage device.

Regarding the paraffin heat storage unit, significant heat transmission occurs between the liquid and solid paraffin. Through thermal conduction, because of the sluggish heat transfer rate and poor heat conductivity, the paraffin shows the horizontal temperature difference being quite great, and the distribution is not uniform. After embedding a metal ring in a spiral, the heat in the horizontal direction can be transferred to the nearby solid paraffin through the spiral metal ring, which effectively supplements the paraffin wax's poor thermal conductivity and minimizes temperature differences. Figure 10 shows the melting diagram of paraffin wax near the spiral metal ring; it is evident that the paraffin wax is close to the spiral metal ring and melts faster than other parts, indicating that the spiral metal ring shortens the melting time of the paraffin wax and enhances heat transfer.

4.1.3. Time Optimization in Heat Storage Process. Figure 11 demonstrates how the average temperature of the thermal storage apparatus changes when different thermal source temperatures and filling materials are used. It is evident that even when the heat source temperature is the same, the internal temperatures of the paraffin thermal storage device and the composite thermal storage device are very different, and the composite heat storage device needs to store heat for a longer period of time. When the heat source temperature is 60°C, 65°C, or 70°C, the composite heat storage device completes the heat storage in about 320 min, 240 min, and 220 min, respectively, less time than the paraffin heat storage device. This is primarily because the spiral metal ring significantly increases the equivalent heat conductance of the material composites, which increases the heat storage efficiency of the thermal storage device.

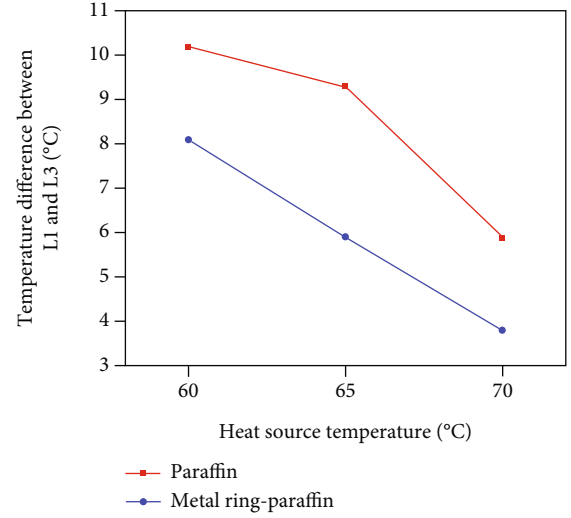


FIGURE 9: Variation diagram of temperature variation along the heat storage device's horizontal axis.



FIGURE 10: Paraffin melting diagram near the spiral metal ring.

The pace for optimization η of the thermal storage device's heat storage duration is given as follows:

$$\eta = \frac{t_p - t_c}{t_p} \times 100\%, \quad (1)$$

where t_p is the duration of a paraffin thermal storage device's thermal storage (min) and t_c is the duration of a composite thermal storage device's thermal storage (min).

Figure 12 demonstrates the optimization rate of the paraffin thermal storage device's thermal storage capacity in comparison to that of the composite heat storage device at various heat source temperatures. As can be seen, incorporating the spiral metal ring may considerably reduce the period that accelerates the rate at which heat is transported by storing and releasing heat. Low heat conductivity of paraffin wax is compensated for by the natural convection of the melted paraffin due to the density difference; when the heat source's temperature increases, the composite thermal storage device's thermal storage time optimization rate reduces. The higher the heat source temperature, the stronger the natural convection, and the smaller the difference in heat

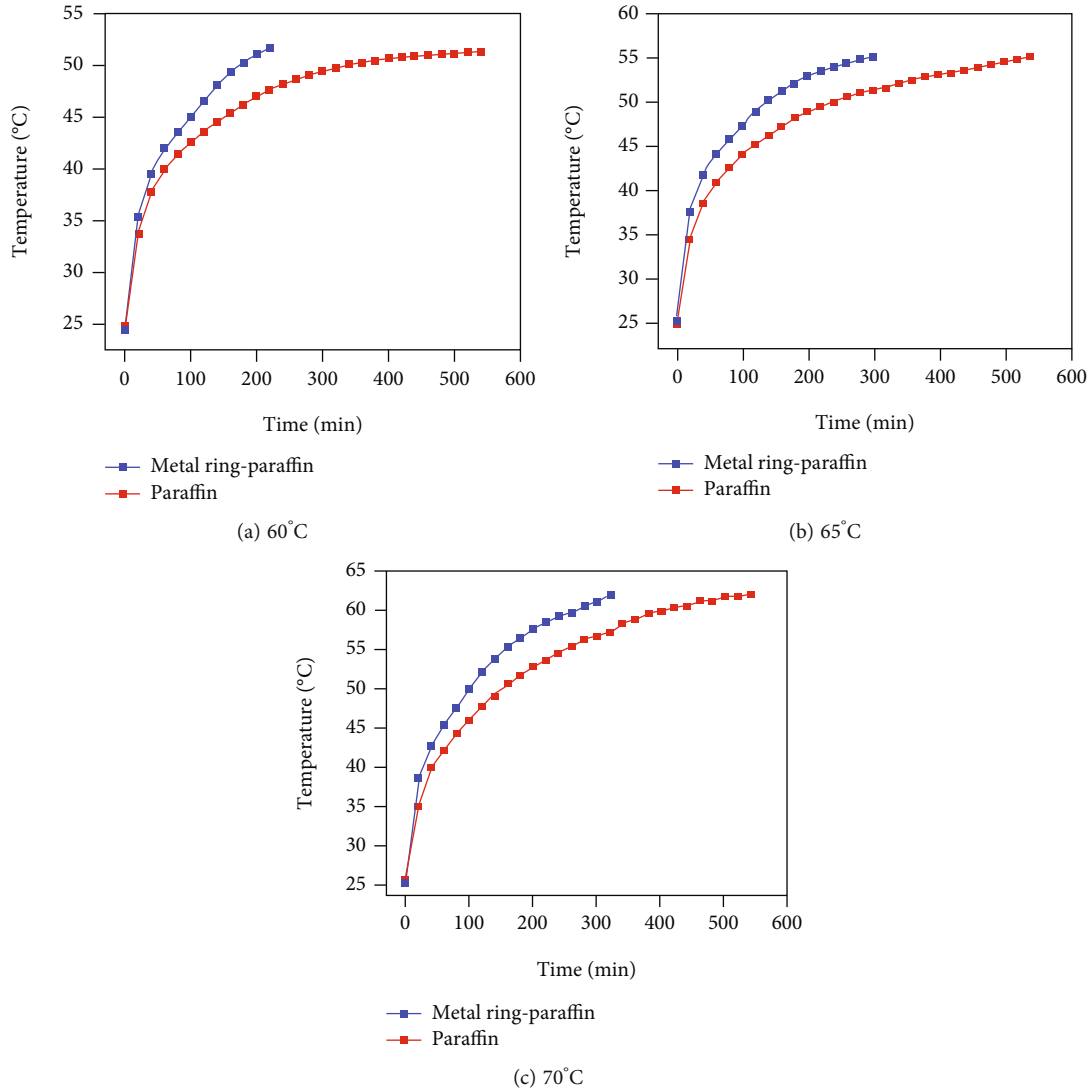


FIGURE 11: Average heat storage device temp change under the condition of various heat source temperatures as well as filling materials.

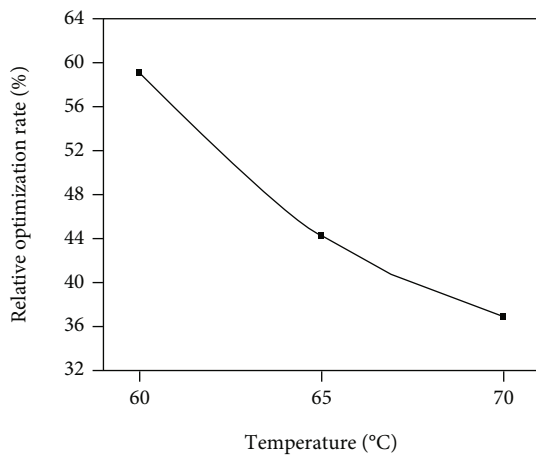


FIGURE 12: Optimization rate the duration of heat storage of a composite heat storage device under different heating source temperatures.

storage time between the paraffin heat storage device, and the relative optimization rate η of heat storage duration is 59.2 percent, 44.4 percent, and 40.7 percent, respectively, at 60°C, 65°C, and 70°C. The optimization impact is stronger when utilizing a low-temperature heat source.

4.1.4. Rate of Heat Transmission during Thermal Storage. If heat loss brought on by the thermal insulation of the thermal storage device is neglected throughout the process of storing heat, the heat transfer rate of the heat exchange fluid may be stated as

$$q = c_{\text{HTF}} M \Delta T_{\text{HTF}}, \quad (2)$$

where, c_{HTF} is the heat transfer fluids' particular heat capacities ($\text{J}/(\text{kg}\cdot^\circ\text{C})$), M is the temperature-transfer fluid volumetric flow rate (kg/s), and ΔT_{HTF} is the difference in temp between thermal exchange fluid's entrance and exit ($^\circ\text{C}$).

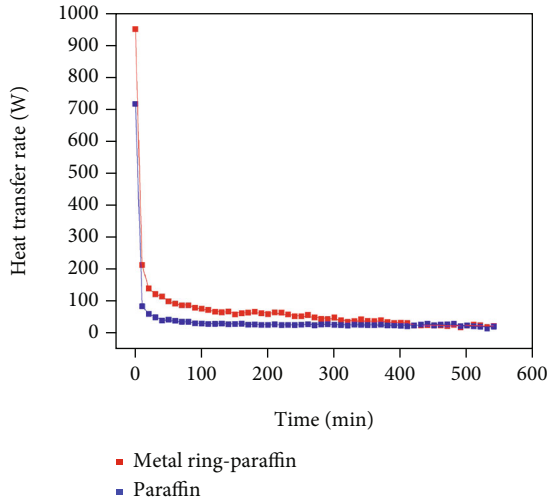


FIGURE 13: Heat transmission rates for various filler materials in heat storage devices.

Figure 13 depicts the thermal transfer rates of composite and paraffin thermal storage devices during the thermal storage process when the heat flux temperature is 70 degrees Celsius. As can be observed, the composite heat storage device’s heat transmission rate is much higher than that of the paraffin heat storage device in the first 200 minutes. The temperature of the heat exchange fluid was high at the start of the heat storage phase and has a higher heat transfer rate than the phase change heat storage material and differs significantly from it. For the paraffin heat storage device, a paraffin liquid film is formed on the outer wall after the paraffin near the outside of the heat flow pipe melts quickly. Because the heat conductivity of liquid paraffin is less than that of solid paraffin, the initial thermal efficiency decreases fast, and the change curve of rate of heat transfer shows a gradual decline after 40 minutes. The heat transfer rate curve for the composite heat storage device is comparable to that of the paraffin device; however, with the addition of the spiral metal ring, the equivalent heat conductivity of the phase change material is significantly enhanced, and its heat transfer rate is considerably greater than that of the paraffin thermal storage device. While a consequence of the phase change material’s slow melting, the thermal storage device’s temperature is increasing as the rate of heat transfer is gradually reducing. After 400 minutes, the heat transfer rate curves of the two devices almost coincide.

Figure 14 depicts when the heating source temperature is temperatures of 60°C, 65°C, and 70°C, the composite heat storage device’s heat transfer rate. It is clear that during the first 0–40 min of the heat storage process, the rate of thermal transfer is high and falls off quickly. This is because at this point, the solid paraffin absorbs heat to melt, and the heat conductivity of the melted paraffin falls, which restricts the transfer of heat and causes the curve to gradually fall until the paraffin is completely melted. The heat transfer rate is likely to be zero, and the average temp of the thermal storage material tends to match that of the heat exchange fluid in the ultimate stage of heat storage. The decreasing trend of the

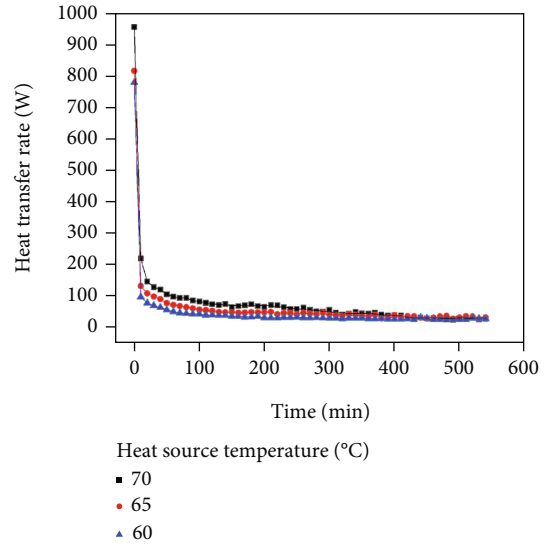


FIGURE 14: Heat transfer rate of heat storage device with a different heat source temperature.

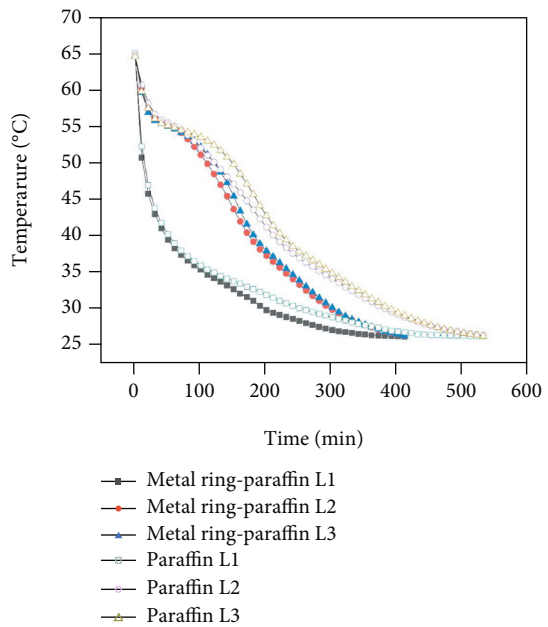


FIGURE 15: Temperature change of various filler materials for a heat storage device throughout the heat release process.

heat transfer rate curves is essentially the same for various heat source temperatures, as can be observed. The ultimate thermal transfer rate curves almost overlap as the thermal source temperature rises, increasing its heat transfer rate.

4.2. Heat Release Process. This research exclusively examines the heat release process under the following experimental conditions: ambient temp with 26°C, starting temperature of thermal storage device of 65°C, and heat exchange fluid flow rate of 0.067 kg/s. Figure 15 demonstrates the temperature change curves for the composite and paraffin heat



FIGURE 16: Physical map of the end of the capillary.

storage devices throughout the heat release procedure. The end system of the indoor heat dissipation capillary is linked to the heat flow pipe during the heat release process, as illustrated in Figure 16. When heat is first released, the water flow in the capillary tube is at room temperature. It then enters the thermal storage device and exchanges heat with the thermal storage-phase altered material. The heat is then released into the air via natural convection between the capillary tube's outer wall and the air. Because the first column of measuring points $L1$ is too close to the heat flow pipe and the temperature changes too fast, there is no obvious phase transition temperature point in the $L1$ temperature change curve. According to the temperature changes of $L2$ and $L3$, it is clear that the temp change curves of composite and paraffin heat storage devices slow down around 20 minutes after the thermal release process begins. During this time, the phase change material releases sensible heat, goes through a phase transition, and starts to emit heat generated. Comparing the composite heat storage device to the paraffin heat storage device, when the phase change material's temperature drops to the phase change point, the temperature drop rate of the latter is significantly faster and the heat release process is completed first, showing that after the paraffin solidifies, the spiral metal ring's enhanced heat conduction-based sensible heat release process can strengthen the heat transfer driving mechanism. The composite heat storage device has a 22.6 percent shorter heat storage period than the paraffin heat storage device.

5. Discussion and Conclusions

Currently, to increase the heating storage device's rate of heat transfer without using external power, three types of mainstream measures to enhance heat transfer are proposed and applied: adding fins on the surface of the heating exchange tube, embedding the phase-change material in a thermal transfer medium having a high heat capacity, and modifying the packaging method for the phase change material [47]; among them, embedding a medium for heat transmission having a high heat capacity is widely used due to the simple operation.

5.1. Selection of Heat Transfer Medium. The technology of embedding enhanced heat transfer media with high thermal conductivity to phase change materials is widely accepted by researchers in the world, such as nonmetallic materials of carbon fiber, silicon powder, and expanded graphite, or foamed metal aluminum and foamed metal copper. However, plus the high cost of carbon fiber, silicon powder, and expanded graphite, they are difficult to be mixed uniformly with phase change materials, and they are even difficult to be separated after being mixed. The metal foam will reduce the volume of thermal storage materials considering its large volume. These problems can result in the high cost of thermal storage systems or reduce thermal storage. In this paper, an ordinary metal iron wire is used to make a spiral metal ring, which has the benefits of compact size, cheap cost, and straightforward operations including making, embedding to, or separating from phase change materials.

5.2. Strengthening Effect of Heat Transfer Medium. The thermal conductivity of the composite phase change material may be increased by including a metal medium with high thermal conductivity into the phase change material with low thermal conductivity and further improve the heat transmission procedure throughout the heat storage and release phase. Heat is mostly transported from the liquid paraffin to the solid paraffin in the paraffin heat storage unit through heat conduction. The sluggish rate of internal heat transmission in paraffin is caused by its poor thermal conductivity. The limited thermal conductivity of paraffin is successfully remedied in this study by embedding a standard spiral metal ring in it, which allows heat to be transmitted to the solid paraffin around it. The heat storage unit's heat storage unit melts faster due to the spiral metal ring's ability to cause the surrounding paraffin to melt sooner and enhancing heat transfer. It has been verified by experiments that this normal spiral metal ring shows a better heat transfer enhancement effect and has good practical application value.

In the experiment, the ratio of the weight of spiral metal ring to paraffin wax will affect the heat storage and release optimization rate of the heat storage unit. The greater the weight of the spiral metal ring, the faster the paraffin melting rate, but at the same time, the heat storage capacity of the unit is also reduced, so there will be a proportion with the highest heat storage and release optimization rate. But that was not studied, given the time constraints of the experiment.

5.3. Using Phase Change Heat Storage in Tunnel Applications. During frigid climates, frost-damaged tunnels [1] will face problems of tunnel icing, water accumulation, and cracking, which seriously threatens operation safety. In China, most of the antifreezing measures for tunnels are passive, and they have problems of poor operation effect and high energy utilization. In order to satisfy the tunnel's heating requirements, the phase change heat storage technology may temporarily store daytime sun energy and release it at nighttime. Cities in the north have heating systems [48, 49] are essential for subway tunnels, which consume a lot of energy. The operational energy consumption of the heating system might be significantly decreased if solar phase change

heating storage technology could be integrated with the heating system used in subway tunnels. No matter whether it is a driving tunnel in a mountain or a subway tunnel in a city, the solar phase-change heat storage engineering can theoretically be combined with the standard heating system in areas that experience extreme cold. When the solar energy is insufficient to suit the need for heating, other auxiliary heat sources can fill in the gap to cut down on the amount of heating energy needed [50–54]. The topic of tunnel heating offers several potential applications for solar phase change heat storage technologies [55–57].

5.4. Conclusions. In this paper, based on the concentric casing type paraffin heat storage device, the spiral metal ring is utilized as the medium for enhancing heat transmission, and the impact of embedding the spiral metal ring on the features of temperature increase and the rate of thermal storage of the thermal storage device is thoroughly examined. The inferences that may be made are as follows:

- (1) When the heat source temperature is 60, 65, or 70 degrees Celsius during the thermal storage process, the unevenness of the temp across the horizontal plane of the heat storage device embedding with the spiral metal ring is reduced by 20.6%, 36.5%, and 35.6%, respectively
- (2) The thermal storage duration of the thermal storage device embedded with the spiral metal ring is decreased by 59.2 percent, 44.4 percent, and 40.7 percent, respectively, at 60°C, 65°C, and 70°C heat source temperatures. When a low-temperature heat source is present, a spiral metal ring's influence on enhancing heat transmission during the thermal storage process is larger
- (3) Heat release time of composite heat storage device embedded with the spiral metal ring is decreased by 22.6 percent when the starting temp of the thermal storage device is 65°C and the ambient temp is 26 degrees

Data Availability

The data used to support the findings of this study are available from the corresponding author upon request.

Conflicts of Interest

No potential conflict of interest was reported by the authors.

Acknowledgments

This research is supported by the Natural Science Foundation of Xinjiang Uygur Autonomous Region (2018D01C081).

References

- [1] M.-Q. Chen, *Study on Thermal Performance of the Phase Change Material Assisted Earth-Air Heat Exchanger*, Chongqing University, 2016.
- [2] B. Li, D.-P. Liu, and L. Yang, "Research progress on thermal storage materials with composite phase change," *Journal of Refrigeration*, vol. 38, no. 4, pp. 36–43, 2017.
- [3] J. Zhao, B.-T. Tang, and S.-F. Zhang, "Progress in studies of organic phase change materials for thermal energy storage," *China Sciencepaper*, vol. 5, no. 9, pp. 661–666, 2010.
- [4] F. Meng, Q.-S. An, and X.-F. Guo, "A review of process intensification technology in thermal energy storage," *Chemical Industry and Engineering Progress*, vol. 35, no. 5, pp. 1273–1282, 2016.
- [5] F.-F. Zhang, Q. Tian, and F.-L. ang Li, "Analysis and optimization on cooling performance of solar ejector refrigeration system with heat storage," *Journal of Huaqiao University (Natural Science)*, vol. 38, no. 4, pp. 525–530, 2017.
- [6] L. Zhao, W. Chen, Q. Li, and W. Wu, "Clean-energy utilization technology in the transformation of existing urban residences in China," *International Journal of Coal Science & Technology*, vol. 8, no. 5, pp. 1138–1148, 2021.
- [7] M. Kenisarin and K. Mahkamov, "Solar energy storage using phase change materials," *Renewable and Sustainable Energy Reviews*, vol. 11, no. 9, pp. 1913–1965, 2007.
- [8] P. Verma and S. K. Singal, "Review of mathematical modeling on latent heat thermal energy storage systems using phase-change material," *Renewable and Sustainable Energy Reviews*, vol. 12, no. 4, pp. 999–1031, 2008.
- [9] B. Zalba, J. M. Marin, L. F. Cabeza, and H. Mehling, "Review on thermal energy storage with phase change: materials, heat transfer analysis and applications," *Applied Thermal Engineering*, vol. 23, no. 3, pp. 251–283, 2003.
- [10] A. Abhat, "Low temperature latent heat thermal energy storage: heat storage materials," *Solar Energy*, vol. 30, no. 4, pp. 313–332, 1983.
- [11] L. Qiu, X.-F. Wu, and M.-Y. Yang, "Research on structure models of the phase change material based energy storage heating floor," *Building Science*, vol. 115, no. 2, p. 41-43+65, 2007.
- [12] W.-S. Hua, X.-L. Zhang, and F. Liu, "Research on the new non-water tank solar collector with PCM heat storage and thermal performance," *Renewable Energy Resources*, vol. 35, no. 3, pp. 395–400, 2017.
- [13] M.-Y. Wang, Y. Liu, and L. Yang, "Heat transfer enhancement of building component with phase change material (PCM) and thermal storage performance of lightweight composite wall," *Building Science*, vol. 35, no. 261 (4), p. 28-35+59, 2019.
- [14] E. M. Sparrow, E. D. Larson, and J. W. Ramsey, "Freezing on a finned tube for either conduction-controlled or natural convection-controlled heat transfer," *International Journal of Heat and Mass Transfer*, vol. 24, no. 2, pp. 273–284, 1981.
- [15] R. G. Kemink and E. M. Sparrow, "Heat transfer coefficients for melting about a vertical cylinder with or without subcooling and for open or closed containment," *International Journal of Heat and Mass Transfer*, vol. 24, no. 10, pp. 1699–1710, 1981.
- [16] K. K. Pillai and B. J. Brinkworth, "The storage of low grade thermal energy using phase change materials," *Applied Energy*, vol. 2, no. 3, pp. 205–216, 1976.
- [17] J. J. Jurinak and S. I. Abdel-Khalik, "On the performance of air-based solar heating systems utilizing phase-change energy storage," *Energy*, vol. 4, no. 4, pp. 503–522, 1979.
- [18] H. G. Lorsch, K. W. Kauffman, and J. C. Denton, "Thermal energy storage for solar heating and off-peak air conditioning," *Energy Conversion*, vol. 15, no. 1-2, pp. 1–8, 1975.

- [19] J. J. Jurinak and S. I. Abdel-Khalik, "Properties optimization for phase-change energy storage in air-based solar heating systems," *Solar Energy*, vol. 21, no. 5, pp. 377–383, 1978.
- [20] D. J. Morrison and S. I. Abdel-Khalik, "Effects of phase-change energy storage on the performance of air-based and liquid-based solar heating systems," *Solar Energy*, vol. 20, no. 1, pp. 57–67, 1978.
- [21] N. W. Hale and R. Viskanta, "Solid-liquid phase-change heat transfer and interface motion in materials cooled or heated from above or below," *International Journal of Heat and Mass Transfer*, vol. 23, no. 3, pp. 283–292, 1980.
- [22] M. Bareiss and H. Beer, "An analytical solution of the heat transfer process during melting of an unfixed solid phase change material inside a horizontal tube," *International Journal of Heat and Mass Transfer*, vol. 27, no. 5, pp. 739–746, 1984.
- [23] D. Feldman, M. M. Shapiro, P. Fazio, and S. Sayegh, "The compressive strength of cement blocks permeated with an organic phase change material," *Energy and Buildings*, vol. 6, no. 1, pp. 85–92, 1984.
- [24] A. K. Bhargava, "A solar water heater based on phase-changing material," *Applied Energy*, vol. 14, no. 3, pp. 197–209, 1983.
- [25] C. J. Ho and R. Viskanta, "Inward solid-liquid phase-change heat transfer in a rectangular cavity with conducting vertical walls," *International Journal of Heat and Mass Transfer*, vol. 27, no. 7, pp. 1055–1065, 1984.
- [26] R. Velraj, R. V. Seeniraj, B. Hafner, C. Faber, and K. Schwarzer, "Experimental analysis and numerical modelling of inward solidification on a finned vertical tube for a latent heat storage unit," *Solar Energy*, vol. 60, no. 5, pp. 281–290, 1997.
- [27] J. C. Choi and S. D. Kim, "Heat-transfer characteristics of a latent heat storage system using $\text{MgCl}_2 \cdot 6\text{H}_2\text{O}$," *Energy*, vol. 17, no. 12, pp. 1153–1164, 1992.
- [28] H.-L. Zhou, *Melting and Solidification Heat Transfer Characteristics of Paraffin in Rectangular Unit and Structure Optimization*, Shandong University, 2020.
- [29] K. Sasaguchi and H. Takeo, "Effect of the orientation of a finned surface on the melting of frozen porous media," *International Journal of Heat and Mass Transfer*, vol. 37, no. 1, pp. 13–26, 1994.
- [30] Y. Zhang and A. Faghri, "Heat transfer enhancement in latent heat thermal energy storage system by using the internally finned tube," *International Journal of Heat Mass Transfer*, vol. 39, no. 15, pp. 3165–3173, 1996.
- [31] G.-P. Ma, *Study on the Structure Design and Mechanism of Heat Transfer Enhancement Embedded in Phase Change Materials Based on Additive Manufacturing*, Dalian University of Technology, 2019.
- [32] H. Yuichi, O. Wataru, and F.-K. Jun, "Thermal response in thermal energy storage material around heat transfer tubes: effect of additives on heat transfer rates," *Solar Energy*, vol. 75, no. 4, pp. 317–328, 2003.
- [33] X. Zhu, Q. Liao, and L.-J. Li, "Effect of additives on thermal energy stored and discharged performance of wax phase change thermal storage with spiral pipe," *Journal of Thermal Science and Technology*, vol. 1, no. 1, pp. 14–19, 2005.
- [34] Y.-K. Lei, Q. Tian, and B. Wu, "Performance test of phase change thermal storage material in radiator heating," *Journal of Thermal Science and Technology*, vol. 40, no. 6, pp. 748–755, 2019.
- [35] A. Siahpush, O. B. James, and J. Crepeau, "Phase change heat transfer enhancement using copper porous foam," *Journal of Heat Transfer*, vol. 130, no. 8, article 082301, 2008.
- [36] S. Mancin, A. Diani, L. Doretto, K. Hooman, and L. Rossetto, "Experimental analysis of phase change phenomenon of paraffin waxes embedded in copper foams," *International Journal of Thermal Sciences*, vol. 90, pp. 79–89, 2015.
- [37] Y. Tian and C.-Y. Zhao, "A numerical investigation of heat transfer in phase change materials (PCMs) embedded in porous metals," *Energy*, vol. 36, no. 9, pp. 5539–5546, 2011.
- [38] Y. Liu, J.-G. Duan, and X.-F. He, "Experiments on enhanced heat transfer performance of low temperature latent thermal energy storage unit," *Acta Energetica Sinica*, vol. 41, no. 6, pp. 335–340, 2020.
- [39] F.-M. Huang, J.-W. Chen, W.-P. Liu, J.-S. Huang, H.-Y. Hong, and W. Chen, "Regional rainfall-induced landslide hazard warning based on landslide susceptibility mapping and a critical rainfall threshold," *Geomorphology*, vol. 408, pp. 108236–108236, 2022.
- [40] Z.-Z. Guo, Y. Shi, F.-M. Huang, X.-M. Fan, and J.-S. Huang, "Landslide susceptibility zonation method based on C5.0 decision tree and K-means cluster algorithms to improve the efficiency of risk management," *Geosciences Frontiers*, vol. 12, no. 6, article 101249, 2021.
- [41] F.-M. Huang, S.-Y. Tao, Z.-L. Chang, J.-S. Huang, S.-H. Jiang, and L. Zhu, "Efficient and automatic extraction of slope units based on multi-scale segmentation method for landslide assessments," *Landslides*, vol. 18, no. 11, pp. 3715–3731, 2021.
- [42] S.-H. Jiang, J. Huang, C. Yao, and J.-H. Yang, "Quantitative risk assessment of slope failure in 2-D spatially variable soils by limit equilibrium method," *Applied Mathematical Modelling*, vol. 47, pp. 710–725, 2017.
- [43] F.-M. Huang, J.-S. Huang, S.-H. Jiang, and C.-B. Zhou, "Landslide displacement prediction based on multivariate chaotic model and extreme learning machine," *Engineering Geology*, vol. 218, pp. 173–186, 2017.
- [44] S.-H. Jiang and J. Huang, "Efficient slope reliability analysis at low-probability levels in spatially variable soils," *Computers and Geotechnics*, vol. 75, pp. 18–27, 2016.
- [45] L.-L. Liu, Y.-M. Cheng, S.-H. Jiang, S.-H. Zhang, X.-M. Wang, and Z.-H. Wu, "Effects of spatial autocorrelation structure of permeability on seepage through an embankment on a soil foundation," *Computers and Geotechnics*, vol. 87, pp. 62–75, 2017.
- [46] S.-H. Jiang and J. Huang, "Modeling of non-stationary random field of undrained shear strength of soil for slope reliability analysis," *Soils and Foundations*, vol. 58, no. 1, pp. 185–198, 2018.
- [47] M. Hawlader, M. S. Uddin, and M. M. Khin, "Microencapsulated PCM thermal-energy storage system," *Applied Energy*, vol. 74, no. 1–2, pp. 195–202, 2003.
- [48] F. Wang and B. Lei, "Energy-saving research on ventilation system of tunnel in subway," *Chinese Journal of Underground Space and Engineering*, vol. 8, no. 1, pp. 172–176, 2012.
- [49] F.-R. Zhang, W.-W. Mao, and M.-Q. Chen, "Research on anti-freezing system of tunnel ground source heat pump based on Trnsys in cold area," *Highway*, vol. 62, no. 8, pp. 265–269, 2017.
- [50] H. Liu, A. Rodriguez-Dono, J. Zhang et al., "A new method for exploiting mine geothermal energy by using functional cemented paste backfill material for phase change heat storage: design and experimental study," *Journal of Energy Storage*, vol. 54, article 105292, 2022.
- [51] Y. Liu, R. Zheng, T. Tian, and J. Li, "Characteristics of thermal storage heat pipe charged with graphene nanoplatelets

- enhanced organic phase change material,” *Energy Conversion and Management*, vol. 267, article 115902, 2022.
- [52] T. Wang, W. Lu, Z. He et al., “Tetradecyl octadecanoate phase change microcapsules incorporated with hydroxylated boron nitrides for reliable and durable heat energy storage,” *Solar Energy*, vol. 245, pp. 127–135, 2022.
- [53] Q. Xia, M. Zhang, H. Gu et al., “Numerical simulation of heat transfer for ₂O₃ composite phase change heat storage particles,” *Journal of Energy Storage*, vol. 52, article 104953, 2022.
- [54] W. Zheng, S. Yang, W. Li, M. Luo, C. Song, and Y. Zhang, “Experimental study on thermal performance of phase change heat storage device with rectangular shell structure,” *Applied Thermal Engineering*, vol. 214, article 118897, 2022.
- [55] W.-V. Liu, D. B. Apel, V. S. Bindiganavile, and J. K. Szymanski, “Analytical and numerical modeling for the effects of thermal insulation in underground tunnels,” *International Journal of Mining Science and Technology*, vol. 26, no. 2, pp. 267–276, 2016.
- [56] X. S. Li, Y. M. Wang, Y. J. Hu, C. Zhou, and H. Zhang, “Numerical investigation on stratum and surface deformation in underground phosphorite mining under different mining methods,” *Frontiers in Earth Science*, vol. 10, 2022.
- [57] F. K. Ali, A. Seyed, and P. H. Faramarz, “Closed-loop bulk air conditioning: a renewable energy-based system for deep mines in arctic regions,” *International Journal of Mining Science and Technology*, vol. 30, no. 4, pp. 511–516, 2020.